



<b>Publication Year</b>	2007
<b>Acceptance in OA</b>	2022-12-27T14:40:05Z
<b>Title</b>	Massive star-formation in G24.78+0.08 studied by means of maser VLBI and thermal interferometric observations
<b>Authors</b>	MOSCADELLI, Luca, Goddi, C., CESARONI, Riccardo, BELTRAN SOROLLA, MARIA TERESA
<b>Publisher's version (DOI)</b>	10.1017/S1743921307012690
<b>Handle</b>	<a href="http://hdl.handle.net/20.500.12386/32805">http://hdl.handle.net/20.500.12386/32805</a>
<b>Serie</b>	PROCEEDINGS OF THE INTERNATIONAL ASTRONOMICAL UNION
<b>Volume</b>	vol. 3, S242

# Massive star-formation in G24.78+0.08 studied by means of maser VLBI and thermal interferometric observations

L. Moscadelli<sup>1</sup>, C. Goddi<sup>2</sup>, R. Cesaroni<sup>1</sup>  
and M. T. Beltrán<sup>3</sup>

<sup>1</sup>INAF, Osservatorio Astrofisico di Arcetri, Largo E. Fermi 5, 50125 Firenze, Italy  
email: mosca@arcetri.astro.it

<sup>2</sup>Harvard-Smithsonian Center for Astrophysics, 60 Garden Street, Cambridge, MA 02138, USA

<sup>3</sup>Departament d'Astronomia i Meteorologia, Universitat de Barcelona, Av. Diagonal 647,  
08028, Barcelona, Catalunya, Spain

**Abstract.** This work presents the results of VLBI observations of 6.7 GHz methanol and 22.2 GHz water masers towards the mm core A in the massive star-forming region G24.78+0.08. Comparing the maser with previous millimeter interferometric and recent continuum VLA observations, the physical properties and the gas kinematics of the G24 A core on linear scales from  $\sim 100$  AU to  $\sim 0.1$  pc are determined.

**Keywords.** Masers, stars: formation, HII regions, techniques: interferometric

---

## 1. Introduction

The star forming region G24.78+0.08 is located at a distance of 7.7 kpc and has a large bolometric luminosity ( $\leq 7 \times 10^4 L_{\odot}$ ). Furuya *et al.* (2002) first detected three molecular cores (in continuum emission at 2 mm) and two HII regions (one of these embedded in one of the cores) spread over  $\sim 0.4$  pc. The region contains at least four distinct centers of star formation, named A, B, C, and D, which Furuya *et al.* (2002) speculate to be in different evolutionary states. Both the molecular core A and the source B have associated HII regions (Codella *et al.* 1997) and, hence, are already ZAMS stars, whereas the other two appear to be less evolved. Cores A and C power bipolar molecular outflows (Furuya *et al.* 2002).

1.4 mm Plateau de Bure Interferometer (PdBI) one-arcsecond angular resolution observations by Beltrán *et al.* (2004) have resolved the structure of the G24 A core into two distinct subcores: G24 A1, towards the southeast (SE), and G24 A2, towards the northwest (NW). G24 A1 is associated with the most compact HII region, while G24 A2 shows strong pointlike emission from 3.6 to 8  $\mu\text{m}$  (GLIMPSE) but weak radio 22 GHz continuum emission. Both G24 A1 and A2 are hot molecular cores (HMCs) (Beltrán *et al.* 2004), with a  $V_{\text{LSR}}$  gradient along a northeast-southwest (NE-SW) direction, approximately perpendicular to the axis of the  $^{12}\text{CO}$  molecular outflow. This fact suggests that the two cores might be rotating around the outflow axis (Beltrán *et al.* 2004). Towards G24 A1 and A2 several species of molecular masers have been detected: 6.7 GHz  $\text{CH}_3\text{OH}$ , observed with the Australian Compact Array (ATCA) by Walsh *et al.* (1998), and 22.2 GHz  $\text{H}_2\text{O}$  and 1.6 GHz OH masers observed with the VLA by Forster & Caswell (1989).

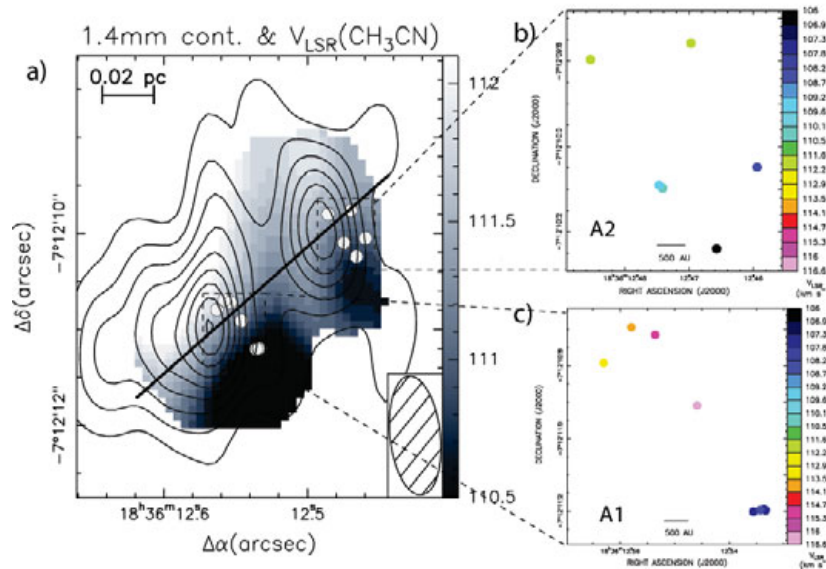


**Figure 1.** a) Map of the CH<sub>3</sub>CN (12 → 11) line peak velocity towards G24 A, with the contour levels in kilometers per seconds indicated in the wedge to the right of the panel (Beltrán *et al.* 2004); overlaid on the CH<sub>3</sub>CN velocity map, is shown the contour map of the 1.4 mm continuum emission (*solid lines*) and the positions of the CH<sub>3</sub>OH 6.7 GHz masers (*filled spheres*); the straight black line represents the axis of the molecular outflow observed with PdBI in <sup>12</sup>CO(1–0) by Furuya *et al.* (2002). b) and c) Positions and line-of-sight velocities of the 6.7 GHz maser features observed towards the subcore A2 and A1, respectively, with the colors (see online version) denoting different line-of-sight velocities, according to the scale on the right-hand side of the panels.

## 2. Observational results

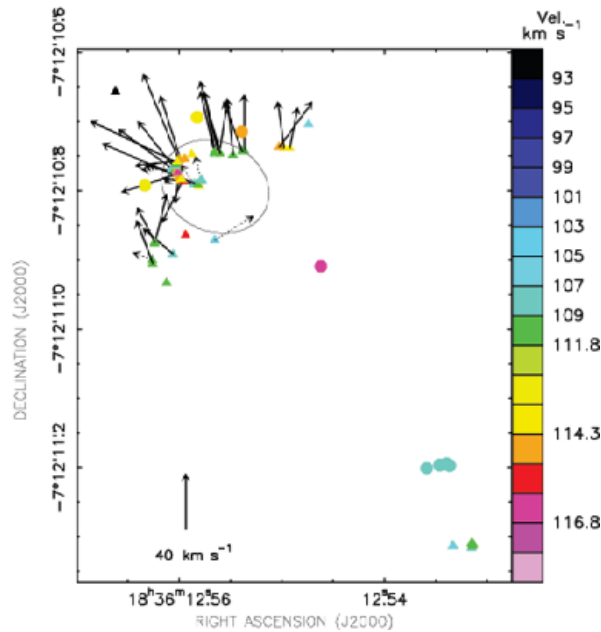
### 2.1. Class II CH<sub>3</sub>OH masers

Figure 1 shows a map of the CH<sub>3</sub>CN (12–11) line line-of-sight velocity overlaid on the contour map of the 1.4 mm continuum emission towards G24 A1 and G24 A2 (Beltrán *et al.* 2004). The absolute positions (accurate to within 50 mas) of the 6.7 GHz methanol masers observed with the EVN are plotted as filled black circles (Fig. 1, panel a). The 6.7 GHz maser emission occurs from two distinct groups of features, each associated with one of the mm subcores (A1 or A2). Both groups of maser features are elongated along a direction that agrees well with the axis of the velocity gradient measured in the CH<sub>3</sub>CN 1.4 mm line.

Panels c and b of Fig. 1 show the line-of-sight velocities of the 6.7 GHz maser features, associated respectively with the A1 and A2 subcores. Across each maser group, the variation of velocities agrees with the velocity gradient observed using the CH<sub>3</sub>CN (12–11) line in the harbouring subcore, with redshifted velocities to the NE and blueshifted velocities to the SW. The methanol maser features are distributed over regions ~three times smaller (0.023 and 0.02 pc) and cover an observed velocity range ~three times larger (9.1 and 5.7 km s<sup>-1</sup>) than the emission of the CH<sub>3</sub>CN thermal line in both subcores.

### 2.2. H<sub>2</sub>O masers

By observing G24.78+0.08 at 22.2 GHz with the VLBA in phase-reference mode at four different epochs, absolute positions and proper motions of the water maser features have been derived. Figure 2 shows the water maser distribution in the subcore A1, which contains the strongest water maser features of the entire G24.78+0.08 region, with



**Figure 2.** Comparison of the distribution of the VLBA 22.2 GHz water (*triangles*) and EVN 6.7 GHz methanol (*dots*) maser features in the mm subcore G24 A1. The colors (see online version) denote different velocities, according to the scale on the right-hand side of the panel. Black arrows show the measured absolute proper motions of water maser features, using dotted arrows to denote the most uncertain measurements; the amplitude scale for proper motions is reported at the bottom of the panel. The ellipse shows the position and the deconvolved FWHM size of the G24 A1 continuum source observed recently in K-band with the VLA by Beltran *et al.* (in preparation).

intensities ranging from  $\approx 0.05$  to  $\approx 100$  Jy beam $^{-1}$ . Maser emission arises from two distinct regions found in the NE and SW corner of the plotted area. The strongest features of the NE maser cluster (called “A1N”) are distributed along an EW line with a length of  $\approx 100$  mas, and along an arc-shaped structure of diameter  $\approx 50$  mas. With a few exceptions, most of the maser features have velocities within  $\pm 5$  km s $^{-1}$  of the LSR systemic velocity (111 km s $^{-1}$ ) of the region. The measured absolute proper motions, with amplitudes in the range 20–60 km s $^{-1}$ , have directions roughly perpendicular to the linear and arcuate spatial distributions of the maser features.

### 3. Rotation and expansion in the mm core G24 A

We now compare the VLBI CH<sub>3</sub>OH and H<sub>2</sub>O maser observations towards the core G24 A with previous millimeter PdBI and recent VLA observations, and discuss a model for explaining the gas kinematics from small (100 AU) to large (0.1 pc) scale.

#### 3.1. Evidence for rotation

Figure 1 shows that, in both cores G24 A1 and A2, the velocity distribution of the methanol 6.7 GHz maser spots agrees well with the velocity gradient measured in the thermal CH<sub>3</sub>CN (12–11) line. If, as suggested by Beltrán *et al.* (2004), the CH<sub>3</sub>CN velocity gradient is due to rotation, the three times larger spread of velocities of the methanol masers across a three times smaller region, might be explained in terms of conservation of angular momentum from large to small scales inside the cores. Assuming that inside the region (of diameter  $\approx 0.02$  pc) traced by the 6.7 GHz maser emission in both cores, the gas is in rotational equilibrium, a dynamical mass of 55 and 19  $M_{\odot}$

for G24 A1 and G24 A2, is derived respectively. From the free-free continuum emission of the ultra-compact HII (UCHII) region in G24 A1, Codella *et al.* (1997) estimate a spectral type of O9.5 for the exciting star, corresponding to a stellar mass of  $\approx 20 M_{\odot}$ . This must be added to the mass of the gas within 0.02 pc from the YSO, which is  $\approx 30 M_{\odot}$  for a mean density of  $10^8 \text{ cm}^{-3}$ . The total mass (star plus gas) is consistent with the mass of  $55 M_{\odot}$  computed from the methanol maser velocity range in G24 A1.

### 3.2. Evidence for expansion

The water maser proper motions measured in the A1N cluster are oriented approximately perpendicular to the geometrical distribution of the maser features, which are mainly concentrated in two structures, a line oriented along the EW direction and an arc (see Fig. 2). The separation from the LSR systemic velocity of the line-of-sight velocities of most maser features of the A1N cluster is quite small ( $\leq 5 \text{ km s}^{-1}$ ) compared with the sky-projected velocity components ( $20\text{--}60 \text{ km s}^{-1}$ ), implying that the velocity vectors of the maser features are close to the plane of the sky. The observed velocity distribution suggests that the A1N water masers are tracing gas *expanding* towards N-NE.

The ellipse drawn in Fig. 2 denotes the position and the deconvolved FWHM size of the continuum source in the G24 A1 core as recently determined using the VLA in K and Q-band by Beltran *et al.* (in preparation). The position of the continuum peak at 22.2 GHz is determined with an accuracy of  $\approx 20 \text{ mas}$ . With an angular resolution of  $\approx 0''.05$ , the continuum source is partially resolved with a deconvolved radius (defined as the geometric mean of the HWHM major and minor axes) of  $0''.07$  (540 AU at a distance of 7.7 kpc). These recent VLA observations confirm that the most likely interpretation for the continuum source is in terms of an UCHII ( $R_{\text{HII}} \leq 0.01 \text{ pc}$ ), that is optically thick at frequencies below 22.2 GHz, becoming optically thin between 22.2 GHz and 44 GHz. The observed continuum flux is consistent with previous observations, indicating a ZAMS spectral type of O9.5 for the central ionizing star.

Figure 2 shows that the UCHII region falls close to the A1N maser cluster. Considering that the estimated size of the HII region is likely an upper limit, most of the water maser features appear to be distributed along the border of the ionized gas. Furthermore, the elongation of the continuum source (P.A. =  $66^{\circ}$ ) agrees well with the average orientation of the water maser proper motions. Thus, the position and the geometry of the continuum source suggests that the water maser motions are driven by the expansion of the ionized gas. Freely expanding ionized gas should move at a maximum velocity comparable to the sound speed in the ionized gas,  $\approx 10 \text{ km s}^{-1}$  assuming a kinetic temperature of  $10^4 \text{ K}$ . The observed velocities of the water masers are significantly higher than  $10 \text{ km s}^{-1}$ , indicating that the ionized gas is *not* freely expanding, but that the expansion must be driven by some additional mechanism than thermal pressure.

Stellar winds are commonly observed towards early-type OB main-sequence stars and observational evidence is being accumulated that such winds play an important role during the early expansion phase of an UCHII region (Hoare *et al.* 2007). A detailed study by Lamers & Leitherer (1993) indicates wind velocities  $V_w = 1500 - 2500 \text{ km s}^{-1}$  and mass loss rates  $\dot{M}_w = 1\text{--}5 \times 10^{-6} M_{\odot} \text{ yr}^{-1}$ , as appropriate for an O9.5 star. Such a powerful stellar wind might be already emitted during the early ZAMS evolution of a massive star. We have considered the case that the expansion of the water maser shell in G24 A1 is driven by a strong wind. Our VLBA water maser and VLA continuum radio observations allow us to set a value for the shell radius and velocity with  $R_0 \approx 500 \text{ AU}$ , and  $V_0 \approx 40 \text{ km s}^{-1}$  respectively. To model the dynamics of the wind-driven shell, we have used equations given in Castor *et al.* (1975) and Shull (1980). A detailed report of our calculations is given in Moscadelli *et al.* 2007 (in preparation). We find that, over the

explored parameter space for the stellar wind properties, and fixing the wind mechanical luminosity, gives a unique value of ambient density for which the wind-driven shell can attain the observed values of radius and velocity. For the likely values of wind luminosities for a O9.5 star, the wind-driven shell models require the hydrogen particle ambient density to lie in the range  $6 \times 10^6 \text{ cm}^{-3} \leq n_{\text{H}} \leq 2.5 \times 10^7 \text{ cm}^{-3}$ . The shell age,  $t_0$ , is predicted to be in the narrow interval  $t_0 = 30\text{--}35 \text{ yr}$ .

### 3.3. Rotation or expansion in the G24 A1 core?

On the basis of the discussed observational evidences, we propose two alternative interpretations to explain the gas kinematics in the G24 A1 core on scales from 100 AU to 0.1 pc.

The expansion detected in the 22.2 GHz water masers on scales of  $\approx 100 \text{ AU}$  (see Fig. 2) might be the dominant motion across the whole molecular core. Thus, the regular variation of line-of-sight velocity observed in the thermal CH<sub>3</sub>CN (12–11) line as well as in the CH<sub>3</sub>OH 6.7 GHz maser emission (see Fig. 1) on linear scales of 0.05 pc, might be due to expansion rather than to rotation, as proposed by Beltrán *et al.* (2004). In particular, the regular velocity gradient can be accounted for only by a *collimated* flow. In this interpretation, the 22.2 GHz water masers would mark the inner portion of a molecular outflow, closer to the YSO and not yet collimated, while the CH<sub>3</sub>OH 6.7 GHz maser and the CH<sub>3</sub>CN thermal emissions would trace the same outflow at larger scale, where collimation is already effective.

Interpreting the motion of the gas in the G24 A1 core in terms of a collimated outflow oriented along the NE–SW direction, apparently contrasts with the PdBI <sup>12</sup>CO(1–0) observations by (Furuya *et al.* 2002), indicating the presence of a bipolar outflow on scale  $\geq 0.1 \text{ pc}$  oriented SE–NW. We propose an alternative scenario, where expansion and rotation can coexist. Figure 2 shows that the detected CH<sub>3</sub>OH 6.7 GHz maser spots are on average more distant from the center of the continuum source than the water maser spots and located beyond the border of the UCHII region. We speculate that methanol masers are tracing the pre-shock ambient gas radiatively heated by the YSO radiation. The value of pre-shock ambient gas density indicated by the wind-driven shell model fits well with the observations of both H<sub>2</sub>O and CH<sub>3</sub>OH masers around the G24 A1 continuum source, since a pre-shock gas density  $n_{\text{H}} \sim 10^7 \text{ cm}^{-3}$  is predicted in the excitation models of both water and methanol masers. The kinematics of methanol masers is expected to differ from that of water masers as the former are located near the G24 A1 core and are unaffected by expansion in the HII region. The water masers should mark the border of the dynamical interaction between the YSO and the surrounding ambient medium: gas moving beyond the water maser shell is not yet perturbed by the YSO evolution (and might be still rotating and slightly contracting), whereas gas inside the maser shell is rapidly expanding due to the YSO wind pressure.

## References

- Beltrán, M. T., Cesaroni, R., Neri, R., *et al.* 2004, *ApJL*, 601, L187  
 Castor, J., McCray, R., & Weaver, R. 1975, *ApJL*, 200, L107  
 Codella, C., Testi, L., & Cesaroni, R. 1997, *A&A*, 325, 282  
 Forster, J. R. & Caswell, J. L. 1989, *A&A*, 213, 339  
 Furuya, R. S., Cesaroni, R., Codella, C., *et al.* 2002, *A&A*, 390, L1  
 Hoare, M. G., Kurtz, S. E., Lizano, S., Keto, E., & Hofner, P. 2007, in *Protostars and Planets V*, ed. B. Reipurth, D. Jewitt, & K. Keil, 181–196  
 Lamers, H. J. G. L. M. & Leitherer, C. 1993, *ApJ*, 412, 771  
 Shull, J. M. 1980, *ApJ*, 238, 860  
 Walsh, A. J., Burton, M. G., Hyland, A. R., & Robinson, G. 1998, *MNRAS*, 301, 640